Supporting information

Electrical and chemical properties of vacancy-ordered lead free layered double perovskite nanoparticles

Amal Sawahreh[1], Tal Binyamin[1], Jie Jiang[2], Oded Millo[3], Oren Goldberg[3], Doron Azulay[3], Ruth Pachter[2], Lioz Etgar[1, *]

[1] Institute of Chemistry, Casali Center for Applied Chemistry and the Center for Nanoscience and Nanotechnology, The Hebrew University of Jerusalem, Jerusalem 91904, Israel.

[2] Air Force Research Laboratory, Materials and Manufacturing Directorate, Wright-Patterson Air Force Base, Ohio 45433, U.S.A.

[3] Racah Institute of Physics, The Hebrew University of Jerusalem and the Center for Nanoscience and Nanotechnology, Jerusalem 91904, Israel.

* Lioz.etgar@mail.huji.ac.il

x	Manganese acetate [mmol]	Cadmium acetate [mmol]
x=1	0	0.18
x=0.8	0.036	0.144
x=0.7	0.054	0.126
x=0.5	0.09	0.09
x=0	0.18	0

Table S1: moles of materials use to synthesize $Cs_4Cd_xMn_{1-x}Bi_2X_{12}$

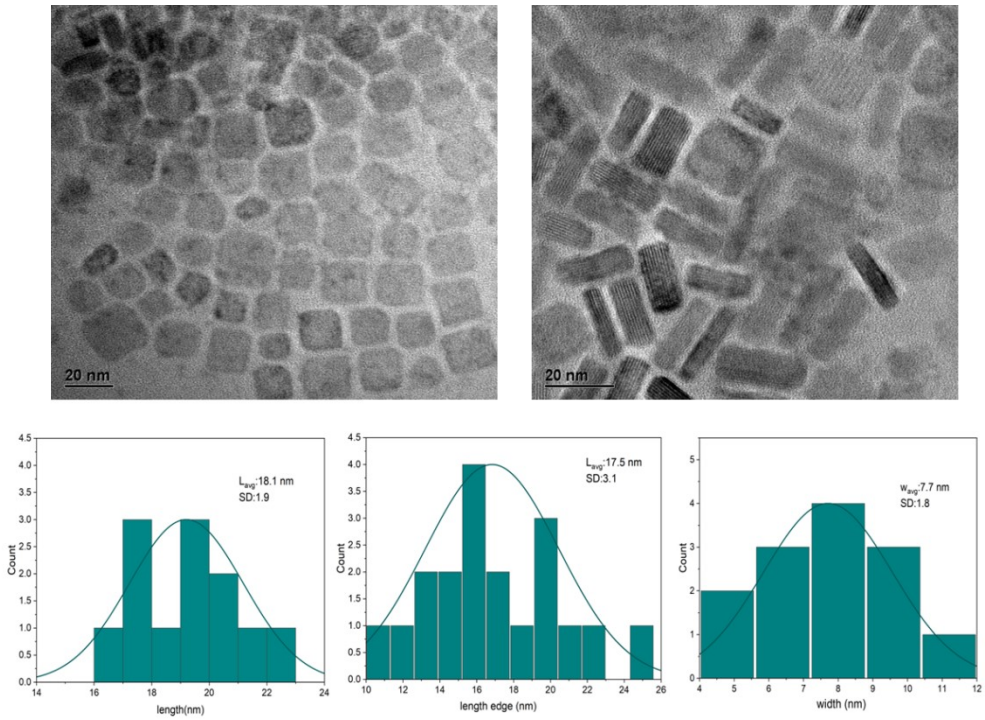

Figure S1: HR-TEM characterization of DLP (x=1) nanoparticle in two different orientations; (a)-zone axis: (1 0 1), (b) zone axis: (1 -1 0). The size distribution histograms of x=1, (c) in zone axis (101) the average length is $18.1 \pm 1.9nm$, (d) in zone axis (1 -1 0) the average edge length is $17.5 \pm 3.1nm$, (f) the average width is $7.7 \pm 1.8nm$.

Table S2: Miller Indices and d-spacing for the different FFT patterns

Cs_3BiCl_6 –zone axis [1 0 1] (figure 4b)			$Cs_4CdBi_2Cl_{12}$ –zone axis [1 0 1] (figure 1c)			$Cs_4CdBi_2Cl_{12}$–zone axis [1 -1 0] (figure 1e)		
(h k l)	d-spacing [nm]	1/d-spacing [1/nm]	(h k l)	d-spacing [nm]	1/d-spacing [1/nm]	(h k l)	d-spacing [nm]	1/d-spacing [1/nm]
1 1 3	0.362	2.762	1 1 0	0.381	2.624	1 1 0	0.380	2.631
-1 3 2	0.255	3.921	2 0 8	0.267	3.733	1 0 2	0.622	1.607
						2 2 0	0.199	5.024

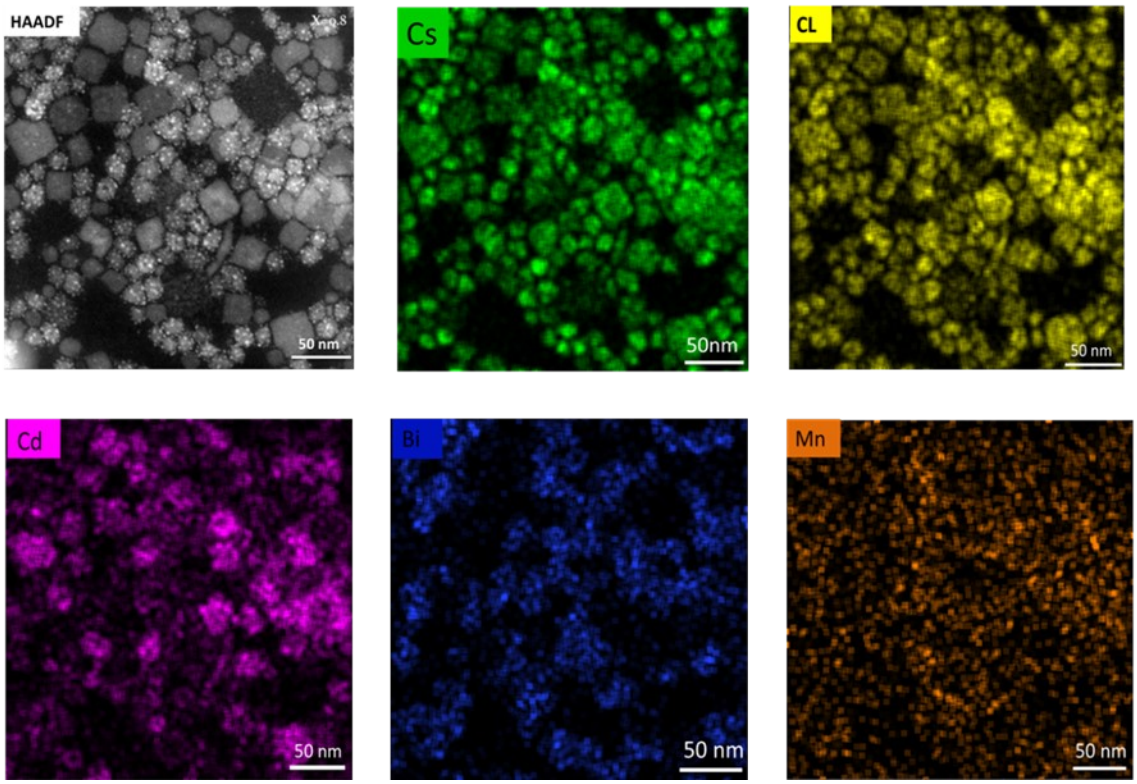

Figure S2: (a) high magnification STEM image $Cs_4Cd_{0.8}Mn_{0.2}Bi_2Cl_{12}$ (x=0.8), (b), (c), (d), (e), (f) STEM-EDS element maps for Cs, Cl, Cd, Bi, Mn; squares show the presence of side product Cs3BiCl6

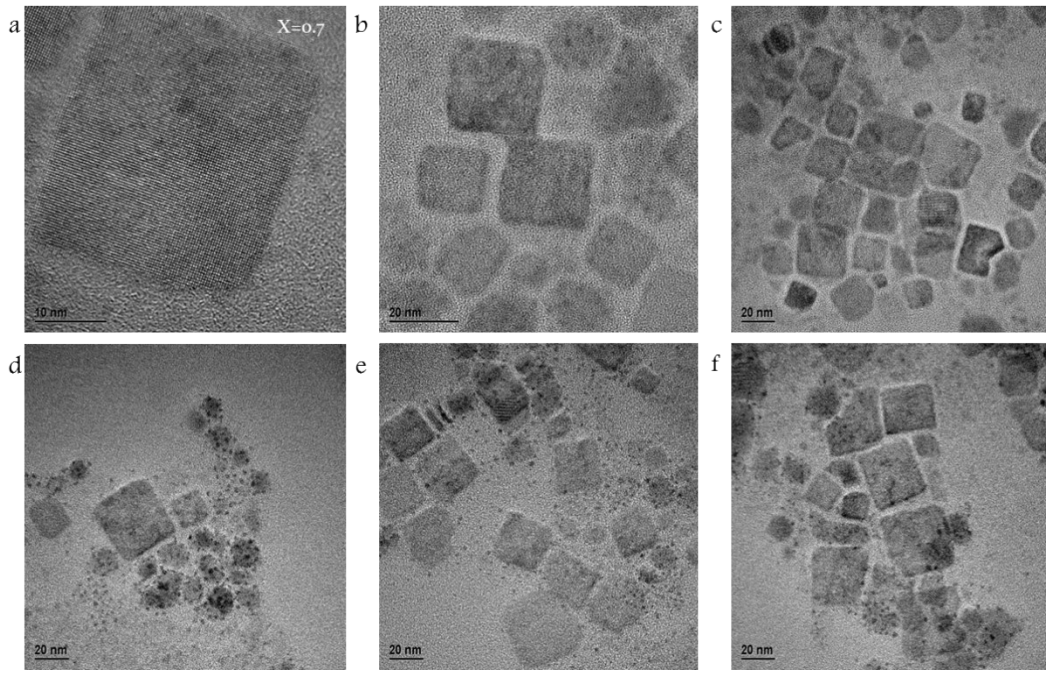

Figure S3: TEM characterization of $Cs_4Cd_{0.7}Mn_{0.3}Bi_2Cl_{12}$ (x=0.7) in different magnifications.

	VBM (ev)	E0 (ev)	Work function (ev)
X=0.8	3.16	14.67	6.53
X=0.5	1.93	14.04	7.16

Table S3: VBM, E0 and work function measured by UPS analysis

Density Functional Theory (DFT) Calculations

Computational details. DFT calculations were carried out with the Vienna ab initio simulation package VASP 5.4.[1] The Kohn-Sham equations are solved using a plane wave basis set with an energy cutoff of 350 eV, and the projector augmented-wave (PAW) potential was applied.[2] A 2×2×2 k-point sampling was used for the 2×2×1 $Cs_4MnBi_2Cl_{12}$ supercell cell. The trigonal $R\bar{3}m$ space group was assumed.[3] The initial spin configuration

for $Cs_4MnBi_2Cl_{12}$ was set as antiferromagnetic state where spins on Mn are parallel along lattice $\vec{b}$ and antiparallel along lattice $\vec{a}$.[4] Upon Cd substitutional doping, the initial spin on dopant Cd is set to zero. The structures were optimized using the PBE functional[5] and the zero damping D3 correction of Grimme,[6] as inclusion of London dispersion in the functional for treating halide perovskites was emphasized,[7] and previously applied.[8] Geometries were fully relaxed regarding lattice parameters and interatomic distances until forces were less than 0.01 eV/Å. In both optimization and electronic structure calculations, spin polarization was included. In the electronic structure calculations for pristine $Cs_4MnBi_2Cl_{12}$, the PBE revised for solids (PBEsol) exchange-correction is adopted.[9]

Figure S4: Two tunneling spectra measured on the NPs marked by asterisk with corresponding colors shown in the topographic image presented in the inset. Both NPs are ~1o nm in lateral dimensions.

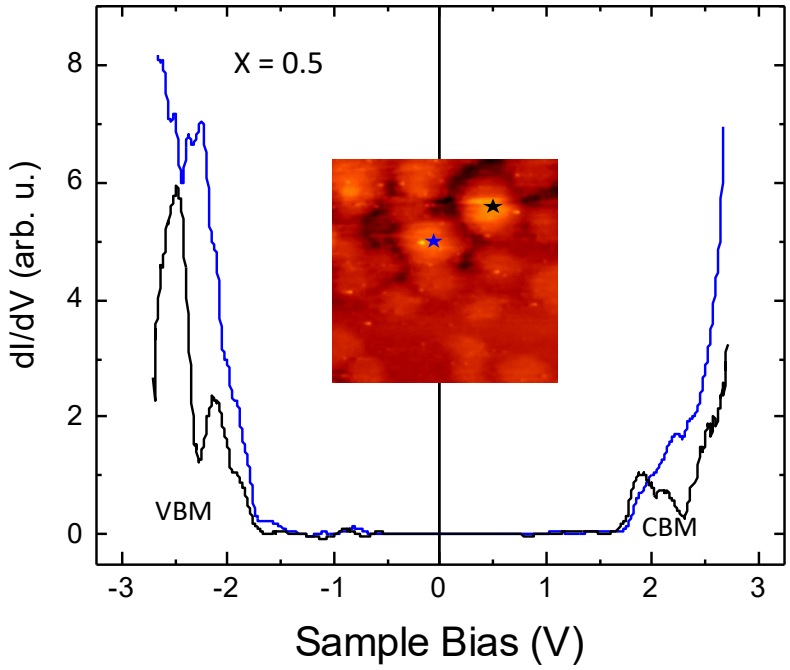

Figure S4: Two dI/dV-V tunneling spectra measured on two different NPs marked by asterisks with corresponding colors shown in the 40×40 nm^2 STM topographic image presented in inset.

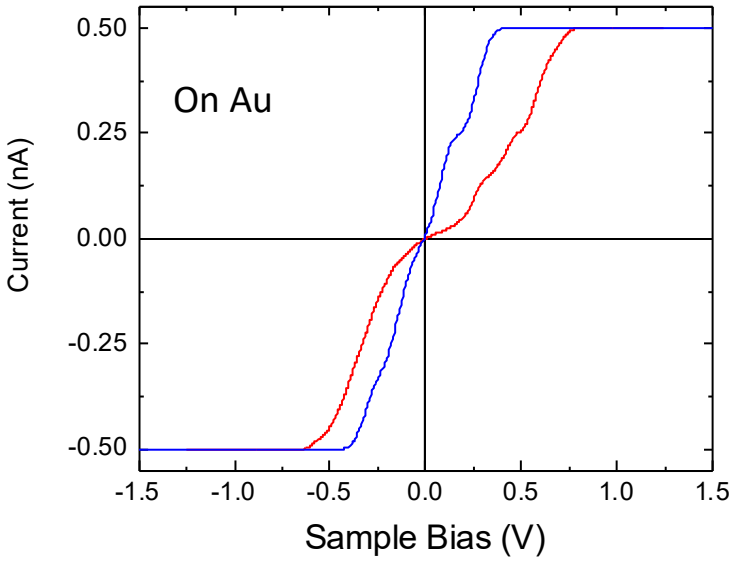

Figure S5: Two I-V characteristics measured on the Au substrate, aside of the NPs, after drop-casting the NPs in chloroform solution.

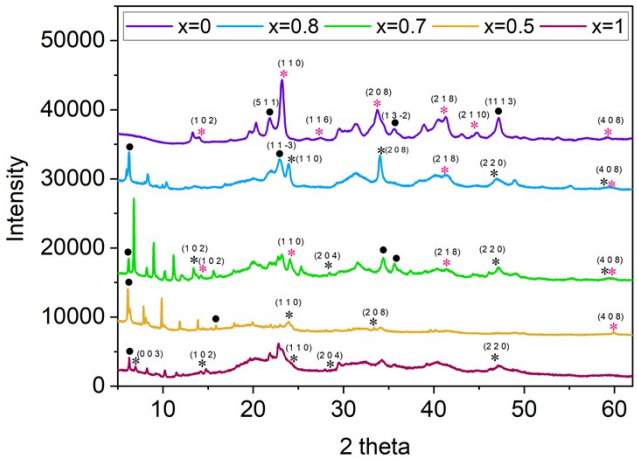

Figure S6: XRD pattern of the nanoparticles which indicate the presence of the desired phases ($Cs_4Cd_xMn_{1-x}Bi_2Cl_{12}$) and Cs_3BiCl_6.

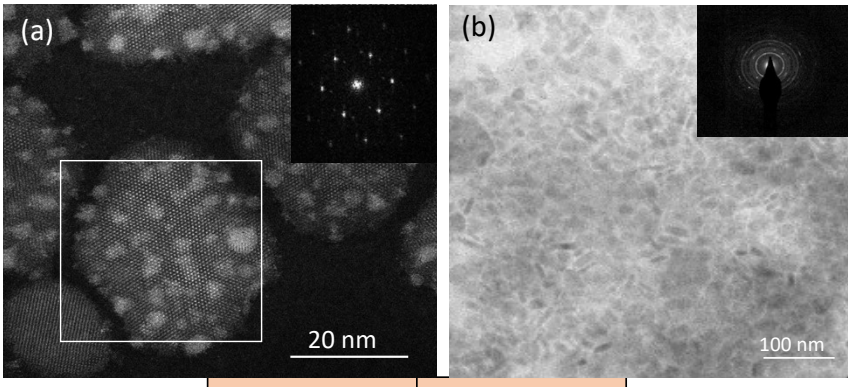

(c) h k l	d-spacing [nm]
(0 1 1)	0.640
(1 1 0)	0.377
(0 2 5)	0.309
(1 2 4)	0.241
(0 3 0)	0.218
(2 2 0)	0.190
(0 4 1)	0.164
(0 4 4)	0.161
(1 3 4)	0.143

Figure S7: HR-TEM image and the corresponding electron diffractions of Cs4CdBi2Cl12 NPs. (a) Zone axis [-1 -1 3] and (b) electron diffraction on larger area and the (c) corresponding h k l crystallographic planes.

References

1. Hafner, J.; Kresse, G., *The Vienna Ab-initio Simulation Program VASP: An efficient and versatile tool for studying the structural, dynamic, and electronic properties of materials*. 1997; p 69-82.
2. Kresse, G.; Joubert, D., From ultrasoft pseudopotentials to the projector augmented-wave method. *Physical Review B* **1999,** *59* (3), 1758-1775.
3. Yang, H.; Shi, W.; Cai, T.; Hills-Kimball, K.; Liu, Z.; Dube, L.; Chen, O., Synthesis of lead-free Cs 4 (Cd 1− x Mn x) Bi 2 Cl 12 (0≤ x≤ 1) layered double perovskite nanocrystals with controlled Mn–Mn coupling interaction. *Nanoscale* **2020,** *12* (45), 23191-23199.
4. Vargas, B.; Torres-Cadena, R. l.; Reyes-Castillo, D. T.; Rodriguez-Hernandez, J.; Gembicky, M.; Menéndez-Proupin, E.; Solis-Ibarra, D., Chemical diversity in lead-free, layered double perovskites: a combined experimental and computational approach. *Chemistry of Materials* **2019,** *32* (1), 424-429.
5. Perdew, J. P.; Burke, K.; Ernzerhof, M., Generalized Gradient Approximation Made Simple. *Physical Review Letters* **1996,** *77* (18), 3865-3868.
6. Grimme, S.; Antony, J.; Ehrlich, S.; Krieg, H., A consistent and accurate ab initio parametrization of density functional dispersion correction (DFT-D) for the 94 elements H-Pu. *The Journal of Chemical Physics* **2010,** *132* (15), 154104.
7. Beck, H.; Gehrmann, C.; Egger, D. A., Structure and binding in halide perovskites: Analysis of static and dynamic effects from dispersion-corrected density functional theory. *APL Materials* **2019,** *7* (2), 021108.
8. Zhang, L.; Liang, W., How the structures and properties of two-dimensional layered perovskites MAPbI3 and CsPbI3 vary with the number of layers. *The journal of physical chemistry letters* **2017,** *8* (7), 1517-1523.
9. Perdew, J. P.; Ruzsinszky, A.; Csonka, G. I.; Vydrov, O. A.; Scuseria, G. E.; Constantin, L. A.; Zhou, X.; Burke, K., Restoring the density-gradient expansion for exchange in solids and surfaces. *Physical Review Letters* **2008,** *100* (13), 136406.
10. Gajdoš, M.; Hummer, K.; Kresse, G.; Furthmüller, J.; Bechstedt, F., Linear optical properties in the projector-augmented wave methodology. *Physical Review B* **2006,** *73* (4), 045112.